INORGANIC CHEMISTRY FRONTIERS

RESEARCH ARTICLE

View Article Online
View Journal | View Issue

Cite this: *Inorg. Chem. Front.*, 2026, **13**, 1913

Homoleptic biisoquinolinedioxide lanthanide complexes for near-infrared circularly polarized luminescence

Douglas Kariuki Mundia, [a] Ashley Schmidt, [b] Jerome R. Robinson, [c] Nathan D. Schley [d] and Gaël Ung *[a]

Received 26th November 2025,
Accepted 13th December 2025

DOI: 10.1039/d5qi02406d

rsc.li/frontiers-inorganic

Near-infrared circularly polarized luminescence (CPL) emitters are of growing interest due to their potential applications in optical telecommunications, bioimaging, and secure information technologies. We report the synthesis and chiroptical properties of lanthanide complexes supported by axially chiral 1,1′-biisoquinoline-*N*,*N*′-dioxide ligands. 8-Coordinate homoleptic complexes composed of a 4 : 1 ligand : metal stoichiometry were obtained. Emissions in the near-infrared I and II windows (900–1700 nm) were observed for both ytterbium and erbium complexes. Although modest quantum yields (6.2% and 3.1%, respectively), and moderate circularly polarized luminescence emission metrics (g_{lum} = ±0.07 and ±0.12, respectively and B_{CPL} = 16.1 M^{-1} cm^{-1} and 3.1 M^{-1} cm^{-1}, respectively) were obtained, the polarization information contained in the CPL spectra combined with a solid-state structure allowed us to assign the symmetry of the complex in solution.

Introduction

The emission of circularly polarized light has garnered recent attention due to promising potential applications in 3D display,[1] encryption,[2] sensing,[3] and telecommunication technologies.[4] The generation of circularly polarized light is straightforward but energy inefficient through optical filtration. The development of direct circularly polarized luminescence (CPL) emitters is thus key to unlock practical applications.

The efficiency of CPL emitters can be quantified by two figures of merit: a dissymmetry factor, g_{lum}, that indicates the degree of polarization of light; and a brightness factor, B_{CPL}, that adds information on the light emitting capabilities. The former can be calculated from experimental data using the following equation: $g_{lum} = \frac{1}{2} \times (I_L - I_R)/(I_L + I_R)$ (where I_L and I_R are the intensities of the left and right circularly polarized light emitted, respectively); while the latter is calculated through the formula: $B_{CPL} = \varepsilon \times \Phi \times g_{lum}$ (where ε is the molar absorptivity and Φ is the quantum yield of the species of interest).[5] Whilst many types of CPL emitters have recently emerged,[6] lanthanide-based CPL emitters have been the most consistent at delivering high metrics.[7]

To date, in lanthanide emitters, high metrics seem to correlate with high symmetry systems: for example, the highest dissymmetry factor (−1.54) at 594 nm from a C_4 symmetrical tetrakis(camphorate) europium(III) complex,[8] and the highest brightness, B_{CPL} (3760 M^{-1} cm^{-1}) at 545 nm from a D_3 symmetrical tris(spinolate) terbium complex.[9] Other high symmetry complexes also exhibit a combination of high metrics.[7] Notably, a D_4 symmetrical dilanthanide complex recently featured high metrics for near-infrared (NIR) CPL.[10] However, in this example, the local C_4 symmetry at the metal centre makes it difficult to discern which symmetry element (local at the metal *vs.* extended for the complex) is responsible for the high metrics. We were interested in investigating this symmetry effect and thus targeted a monometallic D_4 symmetrical species.

Aiming to achieve high dissymmetry factors, we took inspiration from the studies employing axially chiral ligands for CPL.[11–14] Additionally, we were motivated by the work utilizing *N*-oxide ligands for high NIR quantum yields to obtain higher brightness.[15] Owing to the advantages offered by NIR light (reduced scattering, deeper tissue penetration, use in telecommunication) and the scarcity of NIR CPL emitters,[7c] we targeted the axially chiral 1,1′-biisoquinoline-*N*,*N*′-dioxide ligand that we hypothesized could yield an 8-coordinate D_4 symmetrical complex[16] emitting in the NIR region.

We show herein the coordination of axially chiral 1,1′-biisoquinoline-*N*,*N*′-dioxide to lanthanide ions and the (chir)optical properties of the corresponding complexes. We used a combination of solution and solid-state analyses to conclude on the symmetry of the complexes obtained and correlate the chiroptical metrics with structure.

[a]*Department of Chemistry, University of Connecticut, Storrs, Connecticut 06269, USA. E-mail: gael.ung@uconn.edu*
[b]*Brucker AXS LLC, Madison, Wisconsin 53711-5373, USA*
[c]*Department of Chemistry, Brown University, Providence, RI 02912, USA*
[d]*Department of Chemistry, Vanderbilt University, Nashville, Tennessee 37235, USA*

Synthesis and characterization

The targeted 1,1′-biisoquinoline-*N*,*N*′-dioxide (BIQNO) ligand was synthesized from a route adapted from previous reported procedures.[17–19] In summary, racemic BIQNO was obtained by a base-promoted homocoupling of isoquinoline, followed by oxidation using *meta*-chloroperbenzoic acid. Separation of the enantiomers was achieved by generating diastereomeric hydrogen-bonded complexes using enantiopure 1,1′-bi-2-naphthol (Binol). Preferential crystallization of the *S*-BIQNO/*R*-Binol adduct followed by removal of *R*-Binol on a silica column yielded *S*-BIQNO in high enantiopurity (99.4% ee). The enantiomer *R*-BIQNO was isolated using a similar procedure using *S*-Binol (see SI for details).

Coordination to the lanthanides was achieved by reacting 4.05 equivalents of *R*-BIQNO with a lanthanide trifluoromethanesulfonate salt in tetrahydrofuran (THF) (Fig. 1). The complexes were purified by washing off the slight excess of free ligand with cold THF followed by recrystallization in acetonitrile. Complexes of Y, Yb, and Er, were obtained in high yields (91–95%). Purity and stoichiometry were confirmed by combustion analyses (see SI).

In the ^{1}H NMR spectrum of the non-emissive but diamagnetic yttrium complex [Y(*R*-BIQNO)$_4$][OTf]$_3$, a single set of six resonances were observed, consistent with either D_4- and D_2-symmetry in solution. Those resonances are significantly shifted from the free ligand (Fig. 2), confirming binding to yttrium. As expected, the ^{1}H NMR spectrum of the ytterbium and erbium complexes display paramagnetically shifted resonances, ranging from 12.7 to −22.3 ppm and 19.4 to −59.7 ppm, respectively (see Fig. S5 and S8).

Optical and chiroptical properties

The absorption spectrum of the complex displayed a broad band from 300 to 400 nm attributed to a π–π* transition (Fig. 3, dashed blue). The circular dichroism (CD) spectrum of the Yb and Er complexes featured a unique band at 365 nm with a $g_{abs} \sim 0.001$, contrasting with the CD spectrum of the free ligand exhibiting two bands at 327 and 377 nm (Fig. S27–S29). The excitation maximum, recorded for the Yb emission at 980 nm (Fig. 3, dotted black), was red-shifted compared to the maximum absorbance, consistent with a sensitization mechanism.[20]

Upon excitation at 365 nm, the complex [Yb(*R*-BIQNO)$_4$][OTf]$_3$ displayed a luminescence response with a maximum emission peak at 978 nm characteristic of a $^2F_{5/2} \rightarrow {}^2F_{7/2}$ transition (Fig. 3, solid black). Several features due to crystal field splitting are observed, although the signal is relatively narrow compared to other emitters (FWHM = 61.5 nm/~610 cm^{-1}) indicating relatively weak crystal field strength from the ligands. The complex [Er(*R*-BIQNO)$_4$][OTf]$_3$ is also emissive, displaying a typical signal centered at 1535 nm attributed to the $^4I_{13/2} \rightarrow {}^4I_{15/2}$ transition (Fig. S21). Several shoulders arising from crystal field splitting can be observed, albeit with low resolution. The quantum yields were 6.2% and 3.1% for the ytterbium and erbium complexes, respectively.

The singlet and triplet energy levels were determined by synthesizing the analogous gadolinium [Gd(*R*-BIQNO)$_4$][OTf]$_3$ complex. The singlet and triplet levels at 21 970 and 18 300 cm^{-1}, respectively, are relatively higher than the emis-

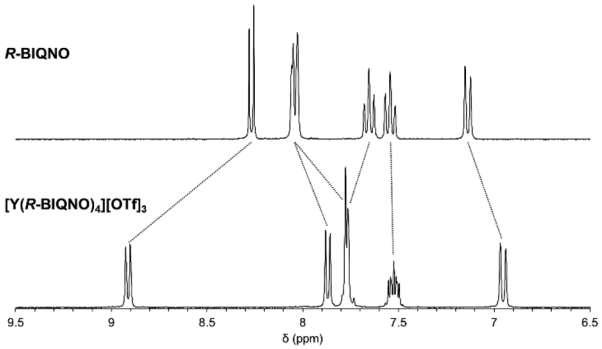

Fig. 2 Aromatic region of the ^{1}H NMR spectra of *R*-BIQNO and [Y(*R*-BIQNO)$_4$][OTf]$_3$ in CD_3CN. See SI for full spectra.

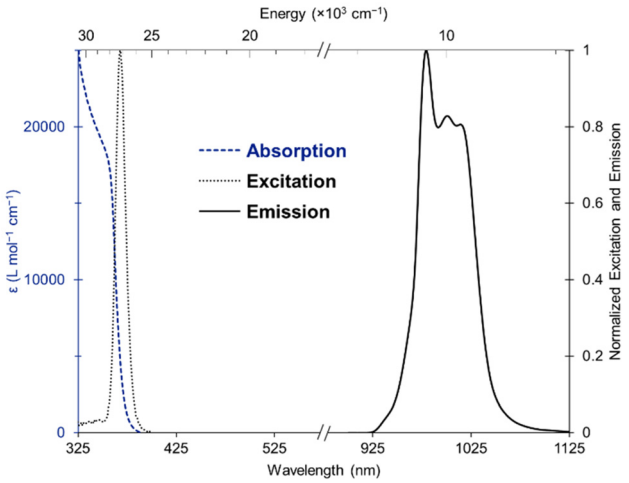

Fig. 3 Absorption (blue dashed), excitation (black dotted), emission (black solid) spectra of [Yb(*R*-BIQNO)$_4$][OTf]$_3$ (160 μM) in 1,2-difluorobenzene.

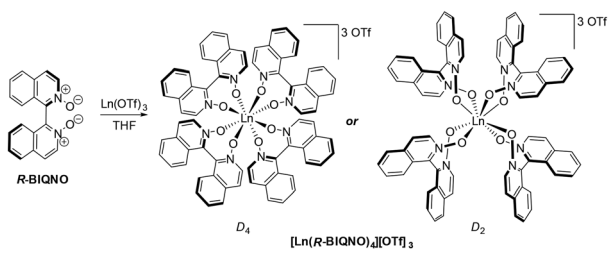

Fig. 1 Synthesis of [Ln(*R*-BIQNO)$_4$][OTf]$_3$ (Ln = Y, Er, Yb). The synthesis of the enantiomeric [Ln(*S*-BIQNO)$_4$][OTf]$_3$ is performed the same way using *S*-BIQNO.

sive levels of both ytterbium and erbium, which is consistent with the low quantum yields observed.

Circularly polarized luminescence spectra of [Yb(*R*/*S*-BIQNO)$_4$][OTf]$_3$ were collected in dilute solutions in 1,2-difluorobenzene, a solvent that we found more adapted to the long exposure times required to acquire CPL data. Fairly well resolved features are seen in the spectra, including a sign inversion at a hot band (attributed to the $2' \rightarrow 0$ transition) around 925 nm and a multisignate pattern between 1000 and 1075 nm (Fig. 4). We note that the $1' \rightarrow 0$ transition and $0' \rightarrow 0$ transition have the same sign, which is unusual compared to other well resolved CPL spectra of high symmetry (C_3, D_3, C_4), which all show an inversion of sign between those transitions. The maximum dissymmetry factor of ±0.07 is obtained at 959 nm (Fig. S25), a significantly lower value than other systems (Table 1 and Table S3), as a result, the CPL brightness B_{CPL} = 16.1 M^{-1} cm^{-1} is also relatively low.

The [Er(*R*/*S*-BIQNO)$_4$][OTf]$_3$ complexes also displayed circularly polarized luminescence (Fig. 5). A trisignate pattern was observed with a maximum g_{lum} of ±0.12 at 1535 nm (Fig. S26). As in the case of the ytterbium complexes, these dissymmetry factors represent relatively small polarization compared to other emitters (Tables 1 and S3). Relatively low brightness were also obtained (B_{CPL} = 3.1 M^{-1} cm^{-1}).

Solid-state studies

Single crystals were grown from vapor diffusion of ether into a solution of [Ln(*R*-BIQNO)$_4$][OTf]$_3$ in acetonitrile. Large clear blocks were obtained, which, despite their apparent quality,

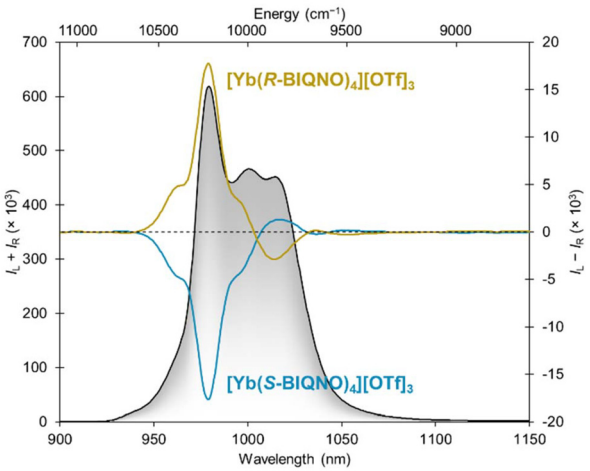

Fig. 4 CPL spectra of [Yb(*S*-BIQNO)$_4$][OTf]$_3$ (blue) and [Yb(*R*-BIQNO)$_4$][OTf]$_3$ (yellow) in solution in 1,2-difluorobenzene (160 μM). The total luminescence is traced in the background. Excitation: 365 nm, bandpass: 10 nm. B_{CPL} determined to be 16.1 M^{-1} cm^{-1}.

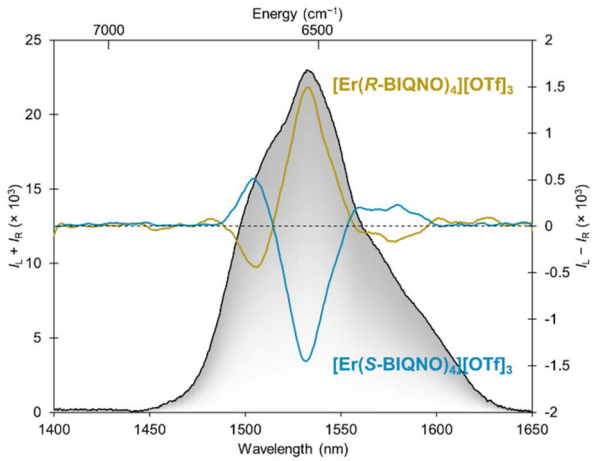

Fig. 5 CPL spectra of [Er(*S*-BIQNO)$_4$][OTf]$_3$ (blue) and [Er(*R*-BIQNO)$_4$][OTf]$_3$ (yellow) in solution in 1,2-difluorobenzene (570 μM). The total luminescence is traced in the background. Excitation: 365 nm, bandpass: 26 nm. B_{CPL} determined to be 3.1 M^{-1} cm^{-1}.

Table 1 Selected[a] summarized optical and chiroptical data for reported NIR-CPL complexes

Complex	Symmetry	ε (M^{-1} cm^{-1})	Φ (%)	τ (μs)	g_{lum}[b] (nm)	B_{CPL} (M^{-1} cm^{-1})	$^{Ln}B_{CPL}$ (M^{-1} cm^{-1})
[Yb(Binol)$_3$][Na]$_3$ [11b]	D_3	26 000	17	—	±0.17 (975)	379	160
[Yb(Sphenol)$_3$][Na]$_3$ [11e]	D_3	17 820	7.5	11.6	±0.22 (973)	146.3	66.0
[Yb(hfbc)$_4$][Cs] [13a]	C_4	—	—	—	±0.38 (988)	—	—
[Yb(^{i}PrPyBox)(TTA)$_3$] [21]	C_1	52 000	0.69	—	±0.029 (972)	5.2	—
[Yb(pydac)(Binol)$_2$][Na] [14]	C_2	27 000	—	2.49 2.06	±0.01 (980)	—	—
[Yb$_2$(BTHP)$_4$] [10]	D_4[c]	—	6.5	14	±0.81 (980)	821	—
[Yb(BIQNO)$_4$][OTf]$_3$	D_2	7474	6.2	35.7	±0.07 (959)	16.1	12.6
[Er(Binol)$_3$][Na]$_3$ [11b]	D_3	42 000	0.58	—	±0.47 (1540)	57.3	22.1
[Er(Sphenol)$_3$][Na]$_3$ [11e]	D_3	19 060	0.28	2.8	±0.77 (1540)	20.7	16.5
[Er(F$_{12}$-Binol)$_3$][K]$_3$ [11d]	D_3	62 000	3.5	10	±0.17 (1526)	184	33.8
[Er(hfbc)$_4$][Cs] [13b]	C_4	34 830	0.07	6.6	+0.83 (1510)	0.23	—
[Er(pybam)$_3$][OTf]$_3$ [22]	D_3	102 000	—	0.21	±0.66 (1519)	—	—
[Er(pybox)$_2$][OTf]$_3$ [23]	C_2	60 000	0.04	4	±0.33 (1539)	0.7	—
[Er(BIQNO)$_4$][OTf]$_3$	D_2	1689	3.1	—	±0.12 (1535)	3.1	1.3

[a] See Table S3 for a complete overview. [b] Values reported in the literature, head-to-head comparisons may not be perfectly accurate due to bandpass differences.[11c,21] [c] C_4 at metal.

diffracted poorly on standard instruments. Using a 2nd generation microfocus source, diffraction patterns at lower angles with brighter spots were obtained. The structure was solved in the non-centrosymmetric $P2_12_12_1$ space group with an unusually large unit cell (14.0 × 25.5 × 44.7 Å). The structures for [Yb(*R*-BIQNO)$_4$][OTf]$_3$ and [Yb(*S*-BIQNO)$_4$][OTf]$_3$ were clearly modulated showing satellite reflections in the diffraction pattern. As a result, the solution given from an average structure displayed smeared ellipsoids, and difficulties in locating the electron density of all of the trifluoromethanesulfonate counterions were encountered. The structure of [Er(*S*-BIQNO)$_4$][OTf]$_3$ could be solved as an average structure, although signs of minor modulation were observed resulting in some elongated ellipsoids. One of the two complexes in the asymmetric unit displayed ellipsoids that we deemed satisfactory to provide reliable bond metrics and angles (Fig. 6).

An 8-coordinate geometry is obtained, intermediate between square antiprism and triangular dodecahedron. The ligands are arranged around the metal in a way that shows only C_2 axes, confirming the D_2 symmetry of the complex. The average M–O bond distance (2.34 Å) is typical for neutral ligands' Ln–O_{neut} bonds but longer than those of anionic ligands (Ln–O_{an} ~ 2.24 Å). This is consistent with the weaker crystal field splitting observed in luminescence, indicative of the weaker binding of the neutral *N*-oxide ligand. Due to the structural similarities between the BIQNO and Binol ligands, we were interested in comparing some of the structural features of the corresponding complexes. The average bite angle O–M–O (72.9°) is smaller compared to that of Binol (81.07°) consistent with both the longer Ln–O bond distances and a more sterically demanding 8-coordinate geometry. A wider torsion angle between the two aryl planes of the BIQNO ligand (67.5°) was also observed relative to that of Binol (62.4°).[11b]

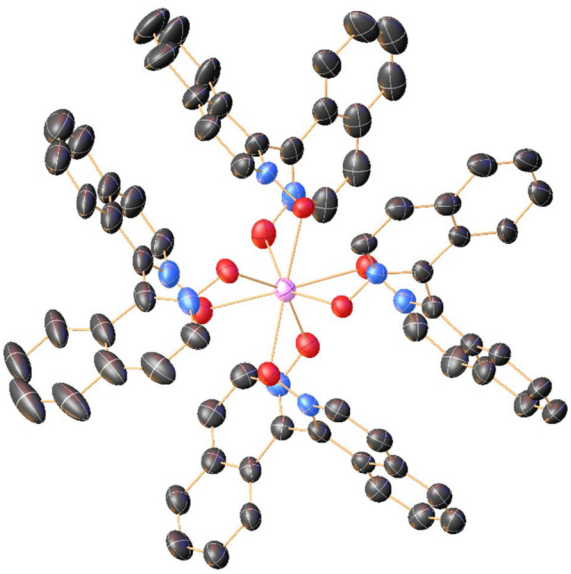

Fig. 6 Structure of [Er(*S*-BIQNO)$_4$][OTf]$_3$ in the solid state. Thermal ellipsoids are drawn at 50% probability. Only one molecule from the asymmetric unit is shown for clarity. Hydrogen atoms and counteranions are omitted for clarity. Pink: erbium, red: oxygen, blue: nitrogen, grey: carbon.

Discussion

Understanding the speciation in solution is key to providing accurate structure/CPL activity relationships that would inform the design of more efficient emitters. Whilst NMR spectroscopy and standard optical spectroscopies were insufficient to determine the symmetry of the [Ln(*R*/*S*-BIQNO)$_4$][OTf]$_3$ complexes in solution (either D_4 or D_2), we leveraged the added resolution provided by CPL spectroscopy to help assign the speciation. The added polarization information (given by the sign of CPL signal) allows for better deconvolution of the transitions between crystal field splitting states (Stark levels). The selection rules of those transitions may thus differ with symmetry (yielding a possible sign change). Examining and comparing the signs of transitions between crystal field splitting states should thus provide clues about the symmetry of the complex.

As mentioned above, the sign of the hot bands in the [Yb(*R*/*S*-BIQNO)$_4$][OTf]$_3$ complexes are inconsistent with the data from other high symmetry complexes. Additionally, the sign and CPL pattern for the [Er(*R*/*S*-BIQNO)$_4$][OTf]$_3$ complexes are reminiscent of a low symmetry C_2 complex.[23] Lastly, the dissymmetry factors are lower than those of high symmetry complexes. Overall, these results suggest that the D_2 symmetry for the [Ln(*R*/*S*-BIQNO)$_4$][OTf]$_3$ complexes is retained in solution, which correlates with the solid-state structure.

We recognize that our comparisons are made with the only few examples available in the literature, which highlights the need for the community to explore more complexes with well-defined symmetries and high-resolution CPL data.

Conclusions

We have successfully synthesized homoleptic lanthanide complexes supported by four enantiopure 1,1′-biisoquinoline-*N*,*N*′-dioxide ligands. Whilst we originally hypothesized the ligands to be suitable to generate D_4 symmetrical complexes, a combination of single crystal XRD analysis, NMR spectroscopy, combustion analyses, and chiroptical spectroscopy allowed us to determine that the complexes were, in fact, D_2 symmetrical. The added resolution provided by CPL spectroscopy was key to assign its symmetry in solution. Whilst the overall CPL metrics are modest, this study provides additional data necessary for a complete understanding of the factors necessary to obtain higher CPL metrics.

Author contributions

DKM: investigation: synthesis, spectroscopy – data curation – writing: original draft; AS: investigation: X-ray diffraction, JRR: investigation: X-ray diffraction; NDS: investigation: X-ray diffraction; GU: conceptualization – funding acquisition – writing: review & editing.

Conflicts of interest

There are no conflicts to declare.

Data availability

The data supporting this article have been included as part of the supplementary information (SI). Supplementary information: experimental details, spectra. See DOI: https://doi.org/10.1039/d5qi02406d.

CCDC 2503942 contains the supplementary crystallographic data for this paper.[24]

Acknowledgements

We thank the University of Connecticut for partial support of this work. This material is based upon work supported by the National Science Foundation under grant no. CHE-2041084.

References

1 M. Schadt, Liquid crystal materials and liquid crystal displays, *Annu. Rev. Mater. Sci.*, 1997, **27**, 305–379.
2 L. E. MacKenzie and R. Pal, Circularly polarized lanthanide luminescence for advanced security inks, *Nat. Rev. Chem.*, 2021, **5**, 109–124.
3 S. Shuvaev, M. A. Fox and D. Parker, Monitoring of the ADP/ATP ratio by induced circularly polarised europium luminescence, *Angew. Chem.*, 2018, **130**, 7610–7614.
4 X. Li, P. L. Voss, J. E. Sharping and P. Kumar, Optical-fiber source of polarization-entangled photons in the 1550 nm telecom band, *Phys. Rev. Lett.*, 2005, **94**, 053601.
5 (*a*) Y. Nagata and T. Mori, Irreverent nature of dissymmetry factor and quantum yield in circularly polarized luminescence of small organic molecules, *Front. Chem.*, 2020, **8**, 448; (*b*) L. Arrico, L. Di Bari and F. Zinna, Quantifying the overall efficiency of circularly polarized emitters, *Chem. – Eur. J.*, 2021, **27**, 2920–2934.
6 (*a*) Y. Zhao, J. Xie, Y. Tian, S. Mourdikoudis, N. Fiuza-Maneiro, Y. Du, L. Polavarapu and G. Zheng, Colloidal chiral carbon dots: an emerging system for chiroptical applications, *Adv. Sci.*, 2024, **11**, 2305797; (*b*) Y. Liu, X. Gao, B. Zhao and J. Deng, Circularly polarized luminescence in quantum dot-based materials, *Nanoscale*, 2024, **16**, 6853–6875; (*c*) T. Zhang, Y. Zhang, Z. He, T. Yang, X. Hu, T. Zhu, Y. Zhang, Y. Tang and J. Jiao, Recent advances of chiral isolated and small organic molecules: structure and properties for circularly polarized luminescence, *Chem. – Asian J.*, 2024, **19**, e202400049; (*d*) J. Chen, Q. Gao, B. Shi, Y. Zhang, T. Wai and Q. Lin, Recent advances in circularly polarized luminescence of planar chiral organic compounds, *Chem. Commun.*, 2024, **60**, 6728–6740; (*e*) Y. Huang, Y. Zhou, X. Guo, Z. Tong and T. Zhuang, Near-infrared circularly polarized luminescence enabled by chiral inorganic nanomaterials, *Nanoscale*, 2025, **17**, 1922–1931; (*f*) X. Zou, N. Gan, Y. Gao, L. Gu and W. Huang, Organic circularly polarized room-temperature phosphorescence: strategies, applications and challenges, *Angew. Chem., Int. Ed.*, 2025, **64**, e202417906; (*g*) X. Wang, W. Yan, D. W. Pang and J. Cai, From synthesis to chiroptical activities: advancements in circularly polarized luminescent inorganic quantum dots, *Nanoscale*, 2025, **17**, 158–186; (*h*) C. Maeda and T. Ema, Recent development of azahelicenes showing circularly polarized luminescence, *Chem. Commun.*, 2025, **61**, 4757–4773; (*i*) V. Kumar, J. L. Páez, S. Míguez-Lago, J. M. Cuerva, C. M. Cruz and A. G. Campaña, Chiral nanographenes exhibiting circularly polarized luminescence, *Chem. Soc. Rev.*, 2025, **54**, 4922–4947; (*j*) M. Ikeshita and T. Tsuno, Recent advances in circularly polarized luminescence (CPL) of chiral boron difluoride complexes, *Phys. Chem. Chem. Phys.*, 2025, **27**, 17116–17129; (*k*) P. Zhao, H. Y. Lu and C. F. Chen, Recent advances in preparation and applications of white circularly polarized luminescent materials, *Chem. Soc. Rev.*, 2025, **54**, 8534–8554.
7 (*a*) F. Zinna and L. Di Bari, Lanthanide circularly polarized luminescence: bases and applications, *Chirality*, 2015, **27**, 1–13; (*b*) H. Y. Wong, W. S. Lo, K. H. Yim and G. L. Law, Chirality and chiroptics of lanthanide molecular and supramolecular assemblies, *Chem*, 2019, **5**, 3058–3095; (*c*) O. G. Willis, F. Zinna and L. Di Bari, NIR-circularly polarized luminescence from chiral complexes of lanthanides and d-metals, *Angew. Chem., Int. Ed.*, 2023, **62**, e202302358; (*d*) A. G. Bispo Jr, N. A. Oliveira, I. M. Diogenis and F. A. Sigoli, Perspectives and challenges in circularly polarized luminescence of lanthanide (III) complexes: from solution-based systems to solid-state applications, *Coord. Chem. Rev.*, 2025, **523**, 216279.
8 M. Tsurui, R. Takizawa, Y. Kitagawa, M. Wang, M. Kobayashi, T. Taketsugu and Y. Hasegawa, Chiral tetrakis Eu(III) complexes with ammonium cations for improved circularly polarized luminescence, *Angew. Chem., Int. Ed.*, 2024, **63**, e202405584.
9 B. A. N. Willis, D. Schnable, N. D. Schley and G. Ung, Spinolate lanthanide complexes for high circularly polarized luminescence metrics in the visible and near-infrared, *J. Am. Chem. Soc.*, 2022, **144**, 22421–22425.
10 L. Wang, Z. Yao, W. Huang, T. Gao, P. Yan, Y. Zhou and H. Li, Remarkable 980 nm circularly polarized luminescence from dinuclear Yb(III) helicates with a D_4 symmetry, *Inorg. Chem. Front.*, 2023, **10**, 3664–3674.
11 (*a*) M. Deng, N. D. Schley and G. Ung, High circularly polarized luminescence brightness from analogues of Shibasaki's lanthanide complexes, *Chem. Commun.*, 2020, **56**, 14813–14816; (*b*) N. F. Mukthar, N. D. Schley and G. Ung, Strong circularly polarized luminescence at 1550 nm from enantiopure molecular erbium complexes, *J. Am. Chem. Soc.*, 2022, **144**, 6148–6153; (*c*) J. A. Adewuyi, N. D. Schley and G. Ung, Vanol-supported lanthanide complexes for strong circularly polarized luminescence at 1550 nm, *Chem. – Eur. J.*, 2023, **29**, e202300800;

(*d*) J. A. Adewuyi and G. Ung, High quantum yields from perfluorinated binolate erbium complexes and their circularly polarized luminescence, *J. Am. Chem. Soc.*, 2024, **146**, 7097–7104; (*e*) D. Schnable and G. Ung, *Inorg. Chem.*, 2024, **63**, 7378–7385.

12 T. Feng, R. Cai, Z. Zhu, Q. Zhou, A. Sickinger, O. Maury, Y. Guyot, A. Bensalah-Ledoux, S. Guy, B. Baguenard, B. Le Guennic and J. Tang, Enhanced near-infrared circularly polarized luminescence activity in fluorinated binolate ytterbium complexes, *Chem. – Eur. J.*, 2025, **31**, e202500910.

13 (*a*) O. G. Willis, F. Zinna, G. Pescitelli, C. Micheletti and L. Di Bari, Remarkable near-infrared chiroptical properties of chiral Yb, Tm and Er complexes, *Dalton Trans.*, 2022, **51**, 518–523; (*b*) O. G. Willis, A. Pucci, E. Cavalli, F. Zinna and L. Di Bari, Intense 1400–1600 nm circularly polarised luminescence from homo- and heteroleptic chiral erbium complexes, *J. Mater. Chem. C*, 2023, **11**, 5290–5296.

14 S. Ruggieri, O. G. Willis, S. Mizzoni, E. Cavalli, M. Sanadar, A. Melchior, F. Zinna, L. Di Bari, G. D. Bisag, M. Fochi, L. Bernardi and F. Piccinelli, Near infrared-circularly polarized luminescence/circular dichroism active Yb(III) complexes bearing both central and axial chirality, *Inorg. Chem.*, 2025, **64**, 5505–5512.

15 C. Doffek and M. Seitz, The radiative lifetime in near-IR-luminescent ytterbium cryptates: the key to extremely high quantum yields, *Angew. Chem., Int. Ed.*, 2015, **54**, 9719–9721.

16 (*a*) T. Saraidarov, R. Reisfeld and M. Pietraszkiewicz, Luminescent properties of silica and zirconia xerogels doped with europium(III) salts and europium(III) cryptate incorporating 3,3′-biisoquinoline-2,2′-dioxide, *Chem. Phys. Lett.*, 2000, **330**, 515–520; (*b*) P. Gawryszewska, O. L. Malta, R. L. Longo, F. R. Goncalves e Silva, S. Alves Jr., K. Mierzwicki, Z. Latajka, M. Pietraszkiewicz and J. Legendziewicz, Experimental and theoretical study of the photophysics and structures of europium cryptates incorporating 3,3′-bi-isoquinoline-2,2′-dioxide, *ChemPhysChem*, 2004, **5**, 1577–1584; (*c*) J.-M. Lehn, M. Pietraszkiewicz and J. Karpiuk, Synthesis and properties of acyclic and cryptate europium(III) complexes incorporating the 3,3′-biisoquinoline 2,2′-dioxide unit, *Helv. Chim. Acta*, 1990, **73**, 106–111; (*d*) J.-M. Lehn and C. O. Roth, Synthesis and properties of sodium and europium(III) cryptates incorporating the 2,2′-bipyridine 1,1′-dioxide and 3,3′-biisoquinoline 2,2′-dioxide units, *Helv. Chim. Acta*, 1991, **74**, 572–578; (*e*) R. O. Freire, M. E. Mesquita, M. A. C. dos Santos and N. B. da Costa Jr., Sparkle model and photophysical studies of europium $BiqO_2$-cryptate, *Chem. Phys. Lett.*, 2007, **442**, 488–491; (*f*) R. Reisfeld, T. Saraidarov, M. Gaft and M. Pietraszkiewicz, Luminescence of cryptate-type Eu^{3+} complexes incorporated in inorganic and ormocer sol–gel matrices, *Opt. Mater.*, 2007, **29**, 521–527; (*g*) P. P. Gawryszewska, M. Pietraszkiewicz, J. P. Riehl and J. Legendziewicz, Investigations of the spectral properties of lanthanide(III) complexes with 3,3′-bi-isoquinoline-2,2′-dioxide ($biqO_2$) and a $biqO_2$-cryptate in solution, solids, and gels, *J. Alloys Compd.*, 2000, **300–301**, 283–288; (*h*) M. Pietraszkiewicz, J. Karpiuk and O. Pietraszkiewicz, Luminescent lanthanide complexes with macrocyclic N-oxides, *Spectrochim. Acta, Part A*, 1998, **54**, 2229–2236; (*i*) P. Gawryszewska, L. Jerzykiewicz, M. Pietraszkiewicz, J. Legendziewicz and J. P. Riehl, Photophysics and crystal structure of a europium(III) cryptate incorporating 3,3′-biisoquinoline-2,2′-dioxide, *Inorg. Chem.*, 2000, **39**, 5365–5372; (*j*) M. Pietraszkiewicz, J. Karpiuk and A. K. Rout, A 3,3′-biisoquinoline-2,2′-dioxide with two dibenzoylmethane side-arms, and its luminescent europium(III) complexes, *J. Coord. Chem.*, 1997, **42**, 207–210; (*k*) M. Pietraszkiewicz, J. Karpiuk, R. Gasiorowski and A. K. Rout, Synthesis and photochemical properties of luminescent Eu(III) complexes with macrocyclic and macropolycyclic ligands incorporating 3,3′-biisoquinoline-2,2-dioxide units, *J. Inclusion Phenom. Mol. Recognit. Chem.*, 1997, **28**, 325–334; (*l*) M. Pietraszkiewicz, J. Karpiuk, R. Gąsiorowski, O. Pietraszkiewicz and A. K. Rout, Luminescent macrocyclic lanthanide complexes bearing N-oxides: potential fluorescent labels for modern medical diagnostics, *Acta Phys. Pol., A*, 1996, **90**, 207–213.

17 W.-W. Xie, Y. Liu, R. Yuan, D. Zhao, T.-Z. Yu, J. Zhang and C.-S. Da, Transition metal-free homocoupling of unactivated electron-deficient azaarenes, *Adv. Synth. Catal.*, 2016, **358**, 994–1002.

18 C. Reep, P. Morgante, R. Peverati and N. Takenaka, Axial-chiral biisoquinoline *N*,*N*′-dioxides bearing polar aromatic C-H bonds as catalysts in Sakurai-Hosomi-Denmark allylation, *Org. Lett.*, 2018, **20**, 5757–5761.

19 M. Nakajima, M. Saito, M. Shiro and S. I. Hashimoto, (*S*,)-3,3′-dimethyl-2,2′-biquinoline *N*,*N*′-dioxide as an efficient catalyst for enantioselective addition of allyltrichlorosilanes to aldehydes, *J. Am. Chem. Soc.*, 1998, **120**, 6419–6420.

20 A. de Bettencourt-Dias, P. S. Barber, S. Viswanathan, D. T. de Lill, A. Rollett, G. Ling and S. Altun, Para-derivatized Pybox ligands as sensitizers in highly luminescent Ln (III) complexes, *Inorg. Chem.*, 2010, **49**, 8848–8861.

21 F. Zinna, L. Arrico and L. Di Bari, Near-infrared circularly polarized luminescence from chiral Yb(III)-diketonates, *Chem. Commun.*, 2019, **55**, 6607–6609.

22 A. Sickinger, B. Baguenard, A. Bensalah-Ledoux, Y. Guyot, L. Guy, F. Pointillart, O. Cador, M. Grasser, B. Le Guennic, F. Riobé, O. Maury and S. Guy, Impact of the experimental bandwidth on circularly polarized luminescence measurements of lanthanide complexes: the case of erbium(III), *J. Mater. Chem. C*, 2024, **12**, 4253–4260.

23 O. G. Willis, F. Petri, G. Pescitelli, A. Pucci, E. Cavalli, A. Mandoli, F. Zinna and L. Di Bari, Efficient 1400–1600 nm circularly polarized luminescence from a tuned chiral erbium complex, *Angew. Chem., Int. Ed.*, 2022, **61**, e202208326.

24 CCDC 2503942: Experimental Crystal Structure Determination, 2025, DOI: **10.5517/ccdc.csd.cc2q1kbp**.